

Pulsations in the atmosphere of the rapidly oscillating star 33 Lib^{★†}

M. Sachkov,^{1‡} M. Hareter,² T. Ryabchikova,^{1,2} G. Wade,³ O. Kochukhov,⁴ D. Shulyak⁵
and W. W. Weiss²

¹*Institute of Astronomy, Russian Academy of Sciences, Pyatnitskaya 48, 119017 Moscow, Russia*

²*Institut für Astronomie, Universität Wien, Türkenschanzstrasse 17, 1180 Wien, Austria*

³*Department of Physics, Royal Military College of Canada, Box 17000, Kingston, Ontario K7K 4B4, Canada*

⁴*Department of Physics and Astronomy, Uppsala University, SE-751 20 Uppsala, Sweden*

⁵*Institute of Astrophysics, Georg-August-University, Friedrich-Hund-Platz 1, 37077 Göttingen, Germany*

Accepted 2011 June 8. Received 2011 June 2; in original form 2011 April 18

ABSTRACT

In 2009, the rapidly oscillating peculiar A-type (roAp) star 33 Lib was the target of an intense observing campaign, combining ground-based spectroscopy with space photometry obtained with the *Microvariability and Oscillation of STars (MOST)* satellite. We collected 780 spectra using the Echelle Spectro Polarimetric Device for the Observation of Stars (ESPaDONs) spectrograph attached at the 3.6-m Canada–France–Hawaii Telescope and 374 spectra with the Fibre-fed Echelle Spectrograph attached at the 2.56-m Nordic Optical Telescope to perform time-resolved spectroscopy of 33 Lib. In addition, we used 111 Ultraviolet and Visual Echelle Spectrograph (UVES) spectra (2004) from the European Southern Observatory archive to check mode stability.

Frequency analysis of the new radial velocity (RV) measurements confirms the previously reported frequency pattern (two frequencies and the first harmonic of the main one) and reveals an additional frequency at 1.991 mHz. The new frequency solution perfectly reproduces the RV variations from the 2004 and 2009 observational sets, providing strong support for p mode stability in this roAp star over at least 5 years.

Key words: stars: atmospheres – stars: chemically peculiar – stars: individual: 33 Lib – stars: magnetic field – stars: oscillations.

1 INTRODUCTION

The rapidly oscillating peculiar A-type (roAp) stars are key objects for asteroseismology, which presently is the most powerful tool for testing theories of stellar structure. Deep within the 3D envelope of a pulsating star, acoustic waves are excited and propagate through regions of varying temperature, density and composition, which influence the wave speed, frequency and direction. Conventional asteroseismology of main-sequence stars has focused on the interpretation of the light and radial velocity (RV) variations produced by these waves as they arrive at the stellar surface, under the assumption of a single surface layer. This is a tremendous limitation, because the complex 3D details of the acoustic wave pattern (e.g. relative phase of waves, radial evolution of wave amplitude, running

versus standing waves, etc.) are nearly impossible to unravel from such simple 2D surface observations. However, the peculiar atmospheres of magnetic roAp stars provide the unique possibility of extending observational asteroseismology to the radial dimension, and to thereby build a complete 3D model of a pulsating stellar atmosphere. This ability is a consequence of the element stratification in Ap star atmospheres (Saio, Ryabchikova & Sachkov 2001; Wade et al. 2001; Ryabchikova et al. 2002; Ryabchikova, Wade & LeBlanc 2003; Kochukhov et al. 2006) where spectral lines of different elements are formed at different heights. Radiative diffusion (Michaud 1970; LeBlanc et al. 2009) in the atmospheres of cool A stars leads to iron-peak elements tending to concentrate in the photospheric layers, while some heavier elements like rare earth elements (REEs) are pushed further out by the radiative force and may produce overabundant ‘clouds’ in the upper atmosphere. This property extends the optical depth range accessible for determining the pulsation velocity by orders of magnitude. This capability has been demonstrated for the roAp stars γ Equ (Kochukhov & Ryabchikova 2001a; Ryabchikova et al. 2002), HR 3831 (Kochukhov 2006), HD 24712 (Ryabchikova et al. 2007a,b) and 10 Aql (Sachkov et al. 2008a).

One of the reasons why oscillations of roAp stars are so important lies in the fact that many oscillation frequencies are excited simultaneously, giving great potential for asteroseismic studies.

[★]Based on observations collected at the European Southern Observatory (ESO), Paranal, Chile (programmes 077.D-0491 and 077.D-0150, retrieved through the ESO archive) and at the Nordic Optical Telescope.

[†]Based on observations obtained at the Canada–France–Hawaii Telescope which is operated by the National Research Council of Canada, the Institut National des Sciences de l’Univers of the Centre National de la Recherche Scientifique of France and the University of Hawaii.

[‡]E-mail: msachkov@inasan.ru

All but one paper on roAp pulsational modelling dealt with the detailed comparison between the observed and non-adiabatic theoretical frequencies for the best-fitting models: α Cir (Bruntt et al. 2009), 10 Aql (Huber et al. 2008), γ Equ (Gruberbauer, Saio & Huber 2008) and HD 101065 (Mkrtychian et al. 2008). These models vary stellar masses, chemical compositions (X , Z , where X and Z are the mass fractions of hydrogen and heavy elements), T - τ relation above the photosphere as well as l value and magnetic field strength. However, for the first time Saio, Ryabchikova & Sachkov (2010) modelled the distributions of the phase and amplitude of RV variations of the roAp star HD 24712 as a function of atmospheric height and compared their results with the observed distributions. The gradual outward increase of phase lag in the outermost layers is well reproduced by theoretical results obtained with a running-wave outer boundary condition. Although the described models agree with most of the observed properties of the oscillations in the atmosphere of HD 24712, no excited oscillation modes with frequencies appropriate for this star were found, e.g. all the modes examined are damped ones. The κ -mechanism does not seem to be strong enough to excite the supercritical high-order p modes in HD 24712.

Based on analytical arguments (see e.g. Sousa & Cunha 2008a) and realistic magnetohydrodynamical simulations of wave propagation in magnetized stellar atmospheres (Khomenko & Kochukhov 2009), pulsation theory argues that in the magnetically dominated regions of the stellar envelope waves are decoupled into orthogonal standing magnetic and running acoustic components. These oscillations are oriented perpendicular and along magnetic field lines, respectively. The total projected pulsation velocity, produced by a superposition of these two components, can have a widely different apparent vertical profile, depending on the magnetic field strength, inclination and the aspect angle. For certain pulsation frequencies, magnetic field parameters and viewing geometries the two components cancel out, creating a node-like structure, or imitating an inwardly running wave.

Observationally, phase jumps in the RV curves, indicating a nodal surface, were discovered in the roAp star 33 Lib by Mkrtychian, Hatzes & Kanaan (2003) and in 10 Aql by Sachkov et al. (2008a). From all roAp stars observed with snapshot spectroscopic time series, only 33 Lib seems to allow for testing the proposed theories of pulsations. Thus, 33 Lib represents a unique laboratory for guiding theoreticians towards a physically consistent model of dynamic roAp star atmospheres. First, pulsations with a single frequency 2014.821 μHz (174.081 d^{-1}) in 33 Lib were detected by Kurtz (1982) from high-speed photometry. Later, Kurtz (1991) found a change of the main frequency to 2014.781 μHz (174.078 d^{-1}) and he also detected the first harmonic of the main frequency. The pos-

sible presence of a second frequency at 1975.21 μHz (170.66 d^{-1}) was indicated but not certain due to poor signal-to-noise ratio (S/N). The possible presence of this unresolved frequency was considered as one of reasons for the observed frequency change in photometry. Kurtz, Elkin & Mathys (2005a) subsequently obtained a 2-h time series of 33 Lib (111 Very Large Telescope/UVES spectra), indicating frequencies undetected in ground-based photometry for which a highly controversial interpretation could be stochastic variations of pulsation amplitudes in the magnetoacoustic boundary layer. The same sort of frequencies appeared in REE lines, and were mainly detected in some other roAp stars by Kurtz, Elkin & Mathys (2006). Kurtz et al. (2005a) confirmed the photometric frequency and its harmonic, and detected a new frequency at 1769 μHz (152.84 d^{-1}) with no confirmation of the frequency at ~ 1975 μHz . A re-analysis of the UVES spectra of 33 Lib (Ryabchikova et al. 2007b) confirmed an observed phase jump between REE II and REE III lines both in RV centre of gravity and bisector measurements across spectral line profiles. The authors also found spectral lines formed close to the position of the nodal zone showing variations at half of the pulsation period.

At the same time, the current observational data are clearly unable to provide an unambiguous picture and confrontation with theory. To resolve this problem, in 2009 we set out to obtain a much longer spectroscopic time series of 33 Lib with simultaneous *Microvariability and Oscillation of Stars (MOST)* photometry. This combination of spectroscopy (which provides 3D resolution of wave propagation as well as a sensitivity to frequencies undetectable photometrically) with the photometry (which provides uninterrupted, very high precision diagnosis of detected pulsation frequencies, allowing for accurate phasing of the spectroscopic data) represents the most sophisticated asteroseismic data set for any roAp star.

2 OBSERVATIONS AND DATA REDUCTION

Spectroscopic monitoring of 33 Lib was performed using the ESPaDOnS spectrograph attached at the 3.6-m Canada–France–Hawaii Telescope (CFHT) during three nights: 2009 May 02, 05 and 11, and with the Fibre-fed Echelle Spectrograph (FIES) attached at the 2.56-m Nordic Optical Telescope (NOT) during five nights: 2009 April 29, May 05, 12, 17 and 21. A total of 780 high-quality spectra were obtained with ESPaDOnS and 374 spectra were obtained with FIES. These spectra were acquired simultaneously with allocated ultraprecise broad-band photometry by the *MOST* mini-satellite, between April 23 and May 22. In addition, we used 111 UVES spectra extracted from the ESO archive to check mode stability. The journal of observations is presented in Table 1, where

Table 1. Journal of observations of 33 Lib.

Start HJD (245 0000+)	End HJD (245 0000+)	Spectral range (\AA)	No. of exposures	Time resolution (s)	Typical S/N	Instr.
53071.763 13	53071.845 98	4960–6990	111	69	100	UVES
54951.527 64	54951.646 01	4766–7364	74	140	80	FIES
54953.894 40	54954.079 97	4950–7200	240	67	90	ESPaDOnS
54957.553 30	54957.671 69	4766–7364	75	140	80	FIES
54957.871 90	54958.052 84	4950–7200	240	67	90	ESPaDOnS
54962.849 50	54963.081 89	4950–7200	300	67	65	ESPaDOnS
54964.542 51	54964.660 90	4766–7364	75	140	80	FIES
54969.511 52	54969.629 90	4766–7364	75	140	80	FIES
54973.500 93	54973.619 41	4766–7364	75	140	80	FIES

the Julian Date of the beginning and the end of each time series, spectral range, number of exposures and S/N ratio are reported.

2.1 Time series ESPaDOnS spectra

Observations of 33 Lib were obtained using ESPaDOnS at CFHT in spectroscopic ‘star-only’ mode. ESPaDOnS is a bench-mounted FIES with optional polarimetric capability. Stellar light collected by the 3.6-m telescope is injected into the fibre within a dedicated Cassegrain module containing all necessary calibration sources. The spectrograph is set up in dual pupil configuration and features a 190-mm pupil, a double set of high-reflectance collimators (cut from a single 680-mm parabolic parent with 1500-mm focal length), a 79 groove mm^{-1} R2 200 \times 400 mm monolithic grating, a fully dioptric $f/2$ camera with 388-mm focal lens and a 210-mm free diameter (seven lenses in four blocks, one of them being a 220-mm quadruplet), a high-dispersion prism cross disperser (made of a train of two identical PBL25Y prisms with 35° apex and 220-mm cross-section) and a CCD detector with $2\text{k} \times 4.5\text{k}$ 0.0135 mm pixels². This design gives a full coverage of the optical spectral domain (from grating order #61 centred at 372 nm to grating order #22 centred at 1029 nm, with three very small gaps: 922.4–923.4, 960.8–963.6 and 1002.6–1007.4 nm) in a single exposure. For more information, see the CFHT official web page for ESPaDOnS.¹

To adequately time-resolve the dominant 8-min pulsation period of 33 Lib, individual exposure times were limited to 35-s exposure duration, with about 32 s for ‘fast’ readout and other overheads (for a total cadence of 67 s per observation). Nominal spectral resolution in this mode is $R = 80\,000$, and the peak S/N of the spectra was approximately 90 per 1.8 km s^{-1} spectral pixel (65 on May 11 due to poorer transparency). A total of $240 + 240 + 300 = 780$ spectral observations were obtained. Observations were reduced using the LIBRE-ESPRIT code (see e.g. Donati et al. 1997) fed through the Upena pipeline at CFHT, yielding optimally extracted, merged, wavelength-calibrated 1D spectra.

2.2 Time series FIES spectra

We have used the FIES at the 2.56-m NOT to perform time-resolved spectroscopy of 33 Lib. The observations were obtained during five nights (April 29, May 05, 12, 17 and 21), for about 3 h each night. We collected 374 stellar spectra using an exposure time of 90 s. With overheads of 48 s, this gave us a sampling rate of approximately one spectrum every 138 s, sufficient to achieve a spectral quality suitable for analysis of the line profile variations with the dominant 8-min pulsation period of this star.

The FIES instrument was configured to use the high-resolution mode, which provides a wavelength coverage of the 4765–7360 Å region at a resolving power of $R = 72\,000$. We used the REDUCE package (Piskunov & Valenti 2002) to perform the standard steps of the echelle spectra calibration (construction of the master flat-field and bias frames, order location, flat-fielding and wavelength calibration) followed by the optimal extraction of the stellar spectra.

The typical S/N of the individual observations is 80 around $\lambda = 5000 \text{ Å}$. The wavelength scale was established with an internal accuracy of $\approx 50 \text{ m s}^{-1}$ using a 2D calibration based on the measured positions of ≈ 1800 emission lines in all echelle orders of ThAr spectra recorded immediately after each sequence of stellar observations.

For both spectroscopic sets, the continuum normalization was carried out in the following way: (a) for each order, data counts are divided by the flat-field blaze function; and (b) for each order, the continuum level is improved iteratively by fitting a smoothing spline function to the highest points in the average spectrum. In addition to this correction, spectroscopic time series were post-processed to ensure homogeneity in the continuum normalization of individual spectra. Extracted spectra were divided by the average spectrum, the resulting ratio was heavily smoothed and then it was used to correct continua in individual spectra. Without this correction, a spurious amplitude modulation of pulsation in variable spectral lines may arise due to an inconsistent continuum normalization.

2.3 MOST photometry

MOST is a Canadian microsatellite in a Sun-synchronous polar orbit, above the terminator, and has an orbital period of ≈ 101 min. It houses a Maksutov telescope with an aperture of 15 cm, a custom broad-band filter (3500–7000 Å) and a CCD detector. A more detailed description of the mission is given by Walker et al. (2003). After the loss of the Tracking CCD in 2006, an image stacking technique was required for the Science CCD, which made it more difficult to fully remove stray light effects. However, it has significantly improved *MOST*’s photometric performance because of the proximity of stars used for tracking to the targets on the same CCD chip (e.g. Guenther et al. 2008).

33 Lib was observed with *MOST* from 2009 April 30 to May 8, but with poor pointing due to problems with one of the reaction wheels. These data were not included in our analysis. *MOST* was pointed back to 33 Lib from 2009 May 20 to 27, with nominal operation of the satellite producing data which were used for the photometric frequency solution referenced in this paper. More details on the data reduction and analysis will be given elsewhere (Hareter et al., in preparation).

3 MODEL ATMOSPHERE, LINE IDENTIFICATION AND RADIAL VELOCITY MEASUREMENTS

A self-consistent model atmosphere of 33 Lib was calculated iteratively with the LLMODELS code (Shulyak et al. 2004) implemented for the magnetic case by Khan & Shulyak (2006) using individual abundances and stratification of Si, Ca, Cr and Fe derived at each iteration. As starting parameters, we adopted $T_{\text{eff}} = 7550 \text{ K}$, $\log g = 4.3$ and the homogeneous abundances derived by Ryabchikova et al. (2004). 33 Lib has rather large overabundances of the REEs; therefore, we included the same extended tables of observed and predicted REE lines as for Przybylski’s star (see Shulyak et al. 2010) in the line opacity calculations. Analysis of the magnetically split lines in 33 Lib spectrum shows that the magnetic field modulus (B) $\sim 5.5 \text{ kG}$; therefore, model calculations as well as all synthetic spectrum calculations were carried out with the magnetic field taken into account. For spectral synthesis, we used SYNTHMAG code (Kochukhov 2007). The final model parameters were derived by comparing the predicted flux distribution with the observed photometry and spectrophotometry. We used the large-aperture *International Ultraviolet Explorer* observations extracted from the International Ultraviolet Explorer Newly Extracted Spectra (INES) data base,² *TD-1* data (Jamar et al. 1976) and spec-

¹ <http://www.cfht.hawaii.edu/Instruments/Spectroscopy/Espadons/>

² <http://sdc.laeff.inta.es/ines/index2.html>

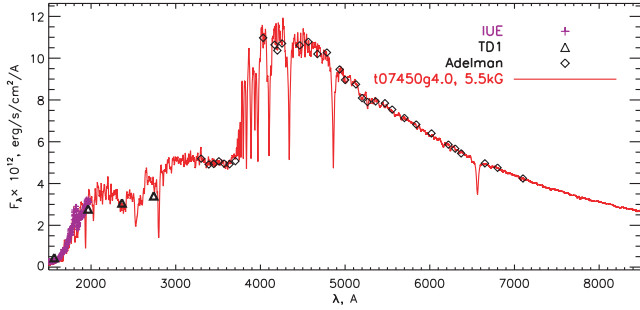


Figure 1. Comparison between the observed (symbols) and theoretical (lines) spectral energy distribution of 33 Lib. The red solid line shows the theoretical energy distribution computed for the final self-consistent model atmosphere with parameters $T_{\text{eff}} = 7450$ K, $\log g = 4.0$ and $\langle B \rangle = 5.5$ kG. The LLMODELS flux spectra are convolved with a FWHM = 10 \AA Gaussian profile.

trophotometric data from the catalogue of Adelman et al. (1989). After three iterations, we derived $T_{\text{eff}} = 7450 \pm 100$ K and $\log g = 3.9 \pm 0.1$ as the best solution for the atmospheric parameters. A fit of the theoretical energy distribution to the observed photometry and spectrophotometry is shown in Fig. 1. With the improved *Hipparcos* parallax $\pi = 11.28 \pm 0.67$ mas (van Leeuwen 2007), we estimated the radius of 33 Lib as $R = 2.09 \pm 0.13 R_{\odot}$, and hence derived a luminosity of $\log(L/L_{\odot}) = 1.08 \pm 0.08$. Within the quoted errors, this value agrees with the $\log(L/L_{\odot}) = 1.18 \pm 0.07$ reported by Balmforth et al. (2001). From the evolutionary tracks, we can estimate a mass of 33 Lib of $1.8 M/M_{\odot}$. These results are in excellent agreement with $\log(L/L_{\odot}) = 1.16 \pm 0.07$ and $M/M_{\odot} = 1.78 \pm 0.06$ found for 33 Lib by Kochukhov & Bagnulo (2006).

To perform a careful line identification and choose lines suitable for pulsation analysis, we have synthesized the whole observed spectral region. Atomic data were extracted from the Vienna Atomic Line Database (Kupka et al. 1999).

The radial velocities were measured with a centre-of-gravity technique. About 100 lines selected in our previous study (Ryabchikova et al. 2007b) were measured for the frequency analysis and the study of the pulsational wave propagation through the stellar atmosphere. When lines of the same ion show similar pulsation phases and amplitudes, we averaged RV measurements to improve further the S/N. The list of the lines is given in Table 2.

4 FREQUENCY ANALYSIS

The RV amplitudes in spectral lines of 33 Lib do not exceed 300 m s^{-1} in the H α -core and Eu II lines, and are even smaller in other lines of REEs. Therefore, the frequency analysis was performed on the RV data of the H α -core and on the averaged RV data of Eu II, Nd II, Nd III and Pr III lines using the SIGSPEC (Reegen 2007) and PERIOD04 (Lenz & Breger 2005) codes. All of the data of ESPaDOnS and FIES were merged and analysed as one data set. A total of nine nights spanning 22 d are available. The PERIOD04 code applies the standard combination of discrete Fourier transform (DFT) and least-squares fitting. The period corresponding to the highest pulsation amplitude was then improved by sine wave least-squares fitting of the RV data, with pulsation period, amplitude and phase treated as free parameters. This fit was removed from the data and then a Fourier analysis was applied to the residuals. This procedure was repeated for all frequencies with a S/N above 4. SIGSPEC calculates the inverse false-alarm probability (spectral significance, see definition of Reegen 2007) for the given frequency range.

Table 2. Summary of the RV pulsational analysis of 33 Lib. Errors in the last digits are given in parenthesis.

Ion	Frequencies detected	Amplitudes (m s^{-1})	Central wavelength of lines used (\AA)
H I	f_1	302(10)	H α -core
	f_2	53(10)	6562
Eu II	f_1	210(9)	6438, 6645
	f_1	85(7)	5546, 5663
Y II	$2f_1$	30(7)	5728
	f_1	90(11)	5164, 5169
Dy II	f_1	40(12)	5730
Tb III	f_1	100(7)	5847, 6092
	$2f_1$	56(7)	6323, 6687
Th III	f_1	190(15)	5375, 6599
La II	f_1	100(9)	5805, 5808, 6100
			6262, 6320, 6399, 6642
Li I	f_1	110(15)	6707
Pr II	f_1	130(8)	5292, 5681, 6165
	$2f_1$	40(8)	
Pr III	f_1	94(3)	5300, 6160, 6866
	$2f_1$	39(3)	7030
	f_2	34(3)	
Nd II	f_3	42(3)	
	f_1	114(4)	5132, 5182, 5277
	$2f_1$	53(4)	5311, 5320, 5486
Nd III	f_2	25(4)	5534, 5804, 6638
	f_3	20(4)	6650
	f_1	78(6)	5051, 5152, 5677
Fe I	$2f_1$	28(6)	5803, 5845, 5851
	f_2	23(6)	6145, 6327
Fe II	f_3	26(6)	
	f_1	25(7)	5424, 5434, 5576
	f_1	30(6)	5414, 5425, 6247

Ultimately, for 33 Lib both codes give very similar frequency solutions. For the final results, we choose the SIGSPEC frequency solution which is given in Table 3. As expected, the highest amplitude frequency $174.074 \pm 0.003 \text{ d}^{-1}$ (or $2014.73 \pm 0.03 \text{ \mu Hz}$) belongs to the principal pulsation period of 8.27 min. Formally, the principal frequency derived by us is slightly shorter than that from photometry, 2014.821 \mu Hz (Kurtz 1991), although they agree within 3σ . We also found the harmonic of the principal frequency in the Nd II, Nd III and Pr III RV data. The second frequency that appears in our RV data is $f_2 = 170.974 \pm 0.005 \text{ d}^{-1}$ or 1978.85 \mu Hz . In the Nd III data, f_2 has a value of 170.97 d^{-1} , while in the Nd II data the value is different by $+0.58 \text{ d}^{-1}$; however, the phases are equal (≈ -3 in both cases). The spectral window (see Fig. 2) shows strong aliasing with 0.22 , 0.78 and 1.0 d^{-1} . The Nd III data have a better point-to-point scatter than the Nd II data; hence, it is more probable that the value of 170.97 d^{-1} , which is also found in the Pr III data, is the correct one. For Nd II and Nd III a phase lag of π is expected because of the observed node (Mkrtichian et al. 2003). To check for phase-dependent aliasing, we subtracted 170.97 d^{-1} from the Nd II residuals after pre-whitening with the principal frequency and its harmonic. Then we added again $f_2 = 170.97 \text{ d}^{-1}$ but with different phases and checked the Fourier transforms. At phases close to -3 (the phase of f_2 in the Nd III data) and $+3.1$ ($\approx \pi$) a peak at 171.55 d^{-1} shows the highest amplitude. This is a strong evidence that 171.55 d^{-1} is an alias, even though the spectral window does not show a pronounced aliasing peak at 0.58 . Fig. 3 illustrates this case. All phases in this section are given in radians.

Table 3. Frequencies for RV data. Errors in the last digits are given in parenthesis.

Label	Frequency (d^{-1})	Significance	Amplitude (m s^{-1})	Phase [$-\pi, \pi$]
Hα-core				
f_1	174.075(4)	117.9	302(10)	-2.895 628
f_2	170.979(17)	6.8	53(10)	-1.726 288
Eu II				
f_1	174.070(6)	61.7	210(9)	0.907 241
Nd II				
f_1	174.075(4)	104.3	114(4)	-1.625 773
$2f_1$	348.147(7)	39.2	53(4)	2.638 426
f_2	171.555(15)	9.8	25(4)	-2.937 492
f_3	155.483(18)	6.5	20(4)	-0.936 600
Nd III				
f_1	174.071(5)	81.6	78(6)	0.133 982
$2f_1$	348.140(12)	14.9	28(6)	1.458 686
f_3	155.727(12)	13.8	26(6)	2.509 509
f_2	170.973(14)	11.3	23(6)	-2.983 738
Pr III				
f_1	174.074(7)	39.2	94(3)	-2.905 973
f_3	155.738(15)	9.4	42(3)	-1.850 699
$2f_1$	348.146(16)	8.0	39(3)	-0.631 134
f_2	170.971(18)	6.7	34(3)	-3.010 928

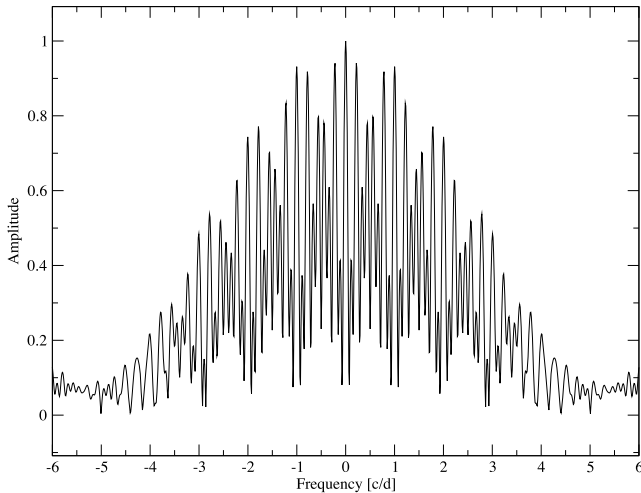


Figure 2. Spectral window of the combined FIES and ESPaDOnS data.

Fig. 4 shows the Fourier transform of the original data, and Fig. 5 shows the Fourier transforms after pre-whitening with the principal frequency and its harmonic. For the Nd II data (the middle panel), the peak at 171.55 d^{-1} is the highest, while in the Nd III data (upper panel) the highest peak in the corresponding range is found at 170.97 d^{-1} . Pre-whitening with f_3 does not change the picture significantly. The same plot for the Pr III data is added for completeness.

The second frequency $f_2 = 170.974 \text{ d}^{-1}$ or $1978.85 \mu\text{Hz}$ is very close to the $\nu \sim 1975 \mu\text{Hz}$, the possible presence of which was suspected by Kurtz (1991) in high-speed photometry. Scaling the H α -core RV amplitudes to match the Kurtz (1991) photometry, we estimate a photometric amplitude of f_2 as $\sim 0.2 \text{ mmag}$, which, in principle, had to be detected. However, pulsation amplitudes of individual modes may grow differently with height in the stellar

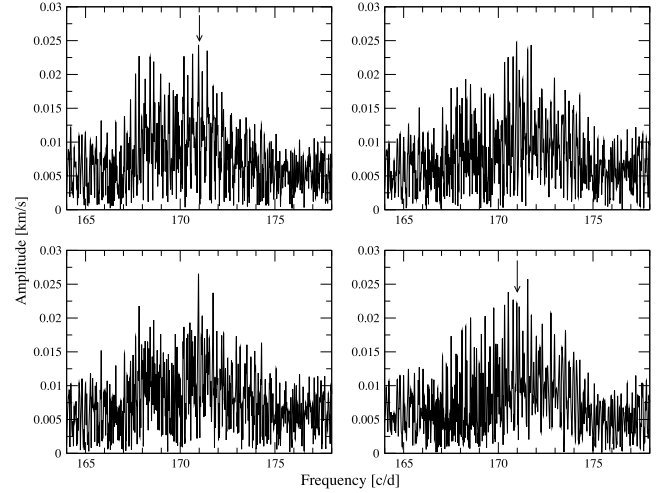


Figure 3. Phase-dependent aliasing. All phases are given in radians. The input frequency is indicated by the arrow. Upper left-hand panel: DFT of the residuals adding f_2 from Nd III without phase lag. Lower left-hand panel: the same but with phase lag +1. Upper right-hand panel: the same but with phase lag +2. Lower right-hand panel: phase lag +3.1 rad ($\approx \pi$).

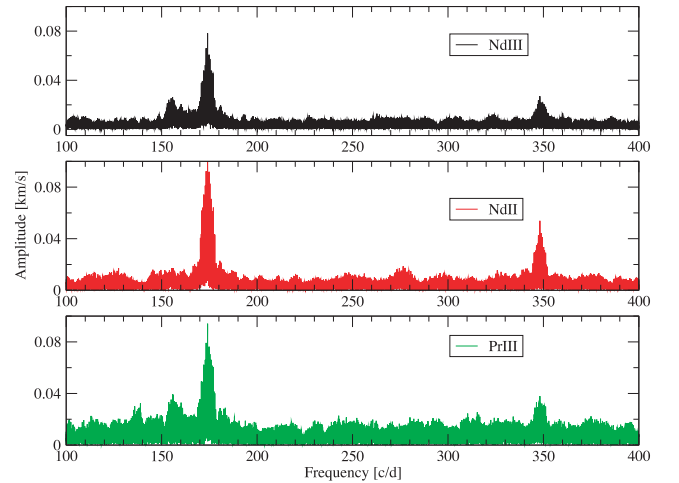


Figure 4. Fourier transforms for the three RV data sets.

atmosphere, and hence scaling factors at the depths of formation of the H α -core and continuum flux may be very different for different modes. The absence of f_2 in Eu II lines – which seem to form deeper than the H α -core in the atmosphere of 33 Lib – supports this hypothesis.

The third frequency $f_3 = 155.75 \text{ d}^{-1}$ (or $1802.6 \mu\text{Hz}$) differs from $\nu = 1769 \mu\text{Hz}$ derived by Kurtz et al. (2005a, 2006) from their 2-h UVES time series. We show below that our present frequency solution provides a good fit to the UVES RV observations.

5 PHASE RELATIONS BETWEEN PHOTOMETRY AND SPECTROSCOPY

Spectroscopic and photometric techniques provide information on the boundary zone relevant for any pulsation model and open access to different modes and hence atmospheric layers. An observed phase lag between luminosity and RV variations is an important parameter required as a first step towards modelling the stellar structure. To determine this phase lag one needs simultaneous photometric and spectroscopic observations, and until now this has been achieved

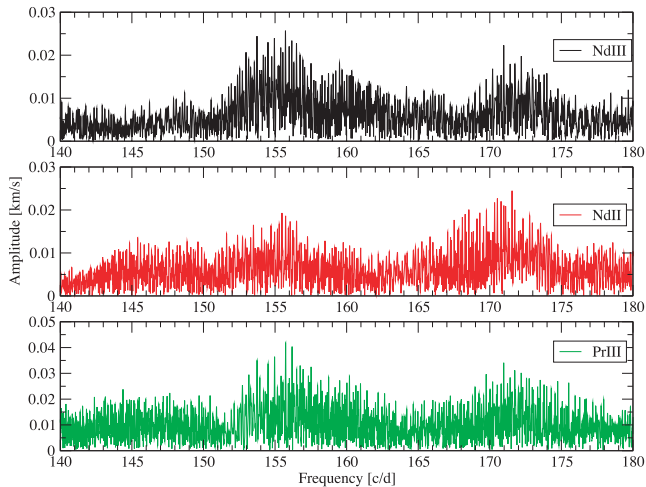


Figure 5. Fourier transforms for the three RV data sets after pre-whitening with f_1 and $2f_1$.

only for three roAp stars: HD 24712 (Ryabchikova et al. 2007a), 10 Aql (Sachkov et al. 2008a) and HD 101065 (Mkrichian et al. 2008). For 33 Lib, our spectroscopic time series were acquired simultaneously with *MOST* photometry. The high S/N and spectral resolution of the present observations of 33 Lib allow us to derive phase lags for individual ions, sampling different atmospheric layers. In order to minimize the influence of the higher (with respect to the spectroscopic observations) point-to-point scatter of the photometric observations, we have constructed an artificial light curve based on the frequencies, amplitudes and phases of the principal frequency and its harmonic as derived by a multisine fit to the *MOST* data (*MOST* team, private communication). As a next step, the artificial photometric time series were cross-correlated with the RV observations. The time interval for the cross-correlation was chosen from +8.27 to −8.27 min (the period of the main frequency, f_1), with an increment of 1 s.

The results of the cross-correlation analysis for the H α -core and for the averaged Eu II, Nd II and Nd III lines are given in Table 4, where we define the phase lag as the difference between the RV maximum and the luminosity maximum, expressed in seconds or as a fraction of the main period $P = 8.27$ min. The error of the phase lag determination was estimated in the following way. We added a normally distributed random signal to both the spectroscopic and photometric data assuming that the noise amplitude corresponds to the observational error. For spectroscopy, the error was derived from the RV determinations, and for photometry the *MOST* team recommended that we use 2 per cent of the signal. A phase lag

Table 4. Phase lags (seconds and fractions of the main period $P = 8.27$ min) between the maxima of RV and luminosity variations of different chemical species in the atmosphere of 33 Lib.

Ion	Phase lag	
	(s)	Period fraction
H I	-20 ± 5	-0.24 ± 0.01
Eu II	-64 ± 8	-0.32 ± 0.01
Nd II	319 ± 9	0.43 ± 0.02
Nd III	74 ± 8	-0.05 ± 0.02

was derived from these noisy data and repeated 200 times. The resulting standard deviation was adopted as the error of the phase lag determination.

6 MODE STABILITY

Pulsation amplitude modulation for roAp stars has been discussed in the literature as a consequence of limited mode lifetime or beating due to close frequencies. Studying γ Equ, the second brightest roAp star, Kurtz (1983) detected a pulsation frequency of $1.339 \mu\text{Hz}$ with an amplitude varying between 0.32 and 1.43 mmag. Beating with a closely spaced frequency has been proposed as the cause of amplitude modulation of this very slowly rotating star (rotation period ~ 77 yr). Libbrecht (1988) discovered two frequencies in γ Equ at 1.366 and $1.427 \mu\text{Hz}$ based on cross-correlation RV analysis in contrast to $1.339 \mu\text{Hz}$ reported earlier by Kurtz (1983). Libbrecht suggested that the amplitude modulation observed in spectra of roAp stars may not be due to closely spaced frequencies, but rather caused by short (~ 1 d) mode lifetimes. Martinez et al. (1996) analysed multisite 1992 campaign data for γ Equ, of 26 nights total duration. They also suggested short lifetimes of pulsation modes because different frequencies appeared in their analysis of individual nights. However, based on continuous photometric observations over 19 days obtained by *MOST*, Gruberbauer et al. (2008) identified seven frequencies including a new one $f_2 = 1.365411 \mu\text{Hz}$ that is very close to the known frequency $f_1 = 1.364594 \mu\text{Hz}$. This discovery explained the puzzling amplitude modulation in γ Equ as beating of two closely spaced frequencies. A common analysis of these *MOST* photometric data and spectroscopic data obtained a year earlier with the Nasmyth Echelle Spectrograph (NES, Panchuk et al. 2009) at the 6-m telescope of the Special Astrophysical Observatory (Russia) results in the conclusion that the excited frequencies of γ Equ are stable on a time-scale of several years because the common photometric/RV frequency solution reproduces the amplitude modulation seen in light and RV curves (Sachkov et al. 2008b).

In another roAp star, 10 Aql, mode stability was confirmed on a time-scale of at least a month or longer (Sachkov et al. 2008a). The authors also showed that short observational data sets (typically 2 h long) do not allow a full resolution of the frequency spectrum of a multiperiodic roAp star.

For 33 Lib, the frequency measurements were obtained by Kurtz (1982, 1991) and Kurtz, Handler & Ngwat (2005b) using high-speed photometry and by Mkrichian et al. (2003) and Kurtz et al. (2005a, 2006) using time series spectroscopy. The frequency solution based on our extensive 2009 data fits perfectly the UVES data obtained 5 years earlier (see Fig. 6). This fact allows us to conclude that modes in 33 Lib are stable on a time-scale of at least 5 years.

Short-time-scale RV amplitude modulation was observed in most of the roAp stars (see Kochukhov & Ryabchikova 2001b; Kurtz et al. 2006). Frequency analysis carried out by Kurtz et al. (2006) resulted in the discovery of the new frequencies seen in spectroscopy but not in the photometry. Since in many cases this modulation cannot be linked to known photometric pulsation frequencies, Kurtz et al. (2006) suggested that such amplitude modulation in spectroscopy means the discovery of a new type of pulsational behaviour in the upper atmospheres of roAp stars, including 33 Lib. They proposed three possible explanations for the newly discovered frequencies: (1) there are modes with nodes near to the level where the photometry samples can be easily detected at the higher level of formation of Pr III lines; or (2) there are higher degree, ℓ , non-radial oblique pulsation modes that are detectable in the spectroscopy because Pr is concentrated towards the magnetic poles where such modes have

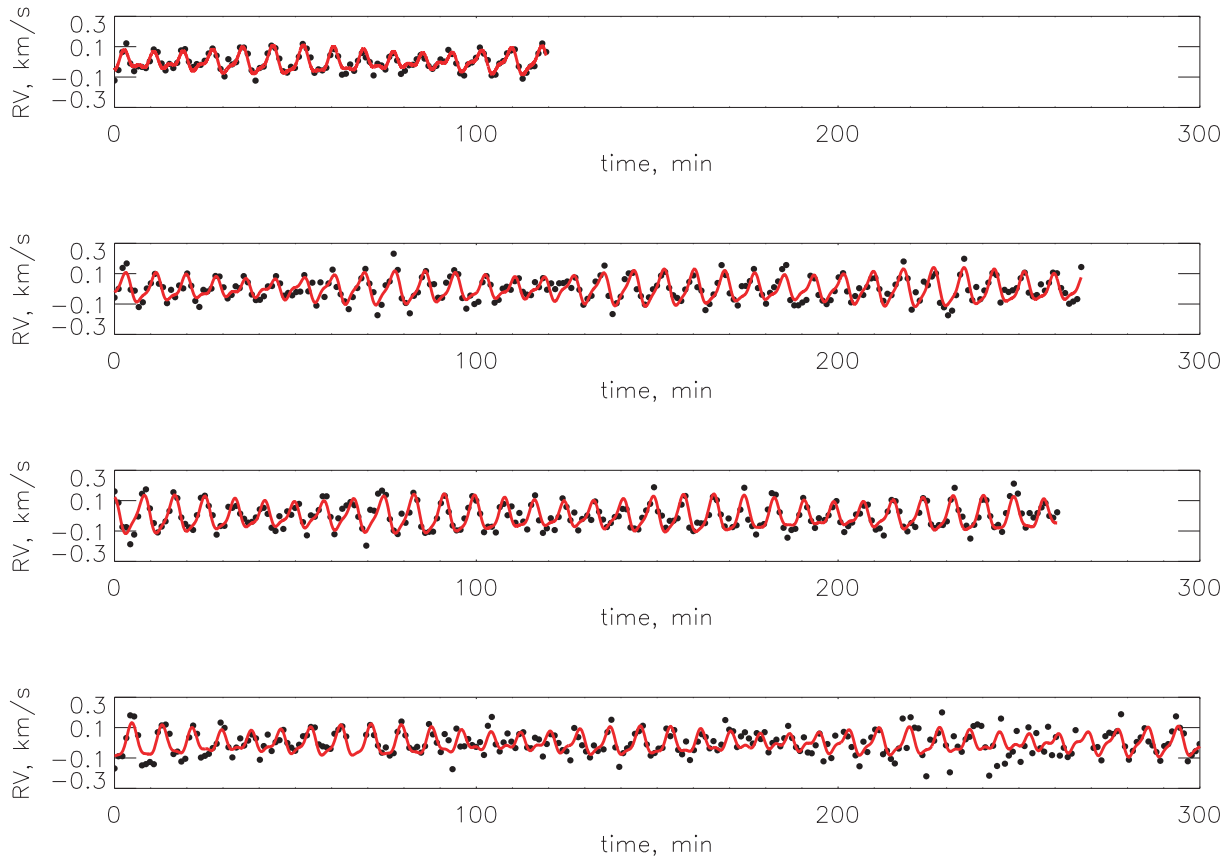


Figure 6. RV curves for Nd III lines for UVES (top) and ESPaDOnS data sets. Theoretical curve with the frequency solution from Table 3 is shown by red solid line.

their highest amplitudes, but average out over the visible hemisphere in the photometry which samples the star’s surface more uniformly; or (3) there is significant growth and decay of the principal mode amplitudes on a time-scale of just a few pulsation cycles at the high level of formation of the Pr III lines and core of the $H\alpha$ line. The latter hypothesis, favoured by Kurtz et al. (2006), is rejected by our conclusion about the long-term stability of pulsation modes.

To explain the difference in frequency solutions derived by Kurtz et al. (2006) and in the present work, we re-analysed the 2003 UVES data and made RV measurements for the same Pr III lines as described by Kurtz et al. (2006). Both frequency solutions were applied to the combined Pr III RV curve. Results of the fitting are shown in Fig. 7, and the RV curve fit parameters are presented in Table 5. Both solutions provide the same quality of fit ($\text{rms} = 27 \text{ m s}^{-1}$) of the RV data. This comparison shows that the time-span of 2 h is simply not sufficient to resolve the $f_2 = 170.971 \text{ d}^{-1}$ frequency that was found in the 2009 data.

7 DISCUSSION

The original motivation of the simultaneous *MOST* photometric and ground-based spectroscopic observations was to take advantage of accurate photometric frequency information in the analysis of spectroscopic data. Note that the high amplitudes of RV variations potentially allow one to obtain mode frequencies even from rather short-duration spectroscopic time series, but with the penalty of an aliasing problem for such data sets with a poor duty cycle. A high duty cycle, on the other hand, is the strength of the continuous

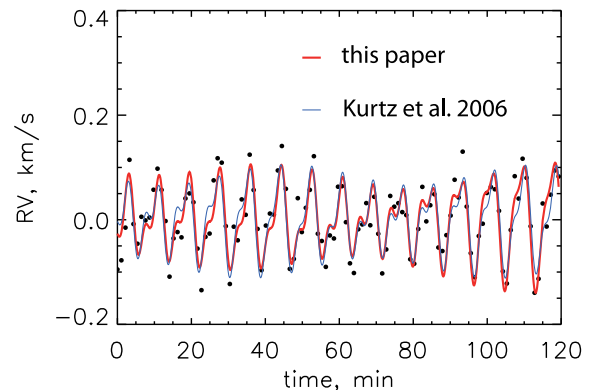


Figure 7. Fit of the combined UVES Pr III RV curve (filled circles) using solutions by Kurtz et al. (2006) (blue thin line) and from the present work (red thick line).

MOST data, but which, on the other hand, suffer from very small photometric amplitudes for more complex modes.

An observed phase lag between luminosity and RV variations is an important parameter for modelling stellar structure. It can be confidently determined only based on simultaneous photometric and RV data. The high S/N and spectral resolution of the present observations of 33 Lib allow us to derive phase lags for individual ions, sampling different atmospheric layers.

Comparison between the results of frequency analysis of the highest quality but short-duration (2 h only) spectroscopic data obtained

Table 5. Fitting parameters of frequency solutions applied to combined Pr III RV curve (UVES 2003 observations)

This work		Kurtz et al. (2006)	
Frequency (d ⁻¹)	Amplitude (m s ⁻¹)	Frequency (d ⁻¹)	Amplitude (m s ⁻¹)
174.074	84	174.096	60
155.738	16	152.842	16
348.146	31	348.142	32
170.971	27		

with the UVES spectrograph on UT2 (Kueyen) and the slightly less accurate but longer duration spectroscopic sets obtained with the ESPaDOnS and FIES spectrographs showed that a 2-h time-span is simply not enough to resolve the new $f_2 = 170.971 \text{ d}^{-1}$ frequency that was found in our data.

Kurtz (1991) proposed that a difference between the main frequency and a suspected frequency at $\sim 1975 \mu\text{Hz}$ may be considered as a large separation $\Delta\nu$, a crucial factor for asteroseismology which is directly connected to the mean density in the star, and describes the separation of consecutive radial overtones for high-order acoustic pulsation (see also Matthews, Kurtz & Martinez 1999). The reality of f_2 is established in our analysis, and thus we may estimate the star’s seismological luminosity and compare it with the luminosity derived from our atmospheric modelling.

The large frequency separation is related to the stellar fundamental parameters (see, for example, equation 4 of Matthews et al. 1999):

$$\Delta\nu = (6.64 \pm 0.36) \times 10^{-16} M^{1/2} T_{\text{eff}}^3 L^{-3/4} \text{ Hz},$$

where M is in solar masses, L in solar luminosities and T_{eff} is in kelvin. Using the 33 Lib parameters determined in Section 3, we compute that $\Delta\nu \approx 57 \mu\text{Hz}$. Our frequency analysis gives $f_1 - f_2 = 36 \mu\text{Hz}$. The asymptotic relation for high-overtone p modes is $\nu_{n\ell} \approx \Delta\nu(n + \ell/2 + \epsilon)$, where n is the radial order, the degree ℓ is the non-radial wavenumber that represents the number of surface nodal lines and ϵ is a constant that depends on the surface properties of the star (Tassoul 1980). If the observed frequency difference corresponds to the separation between consecutive overtones of the same mode, then the seismological luminosity is $\log(L/L_{\odot}) = 0.73$. The value is $\log(L/L_{\odot}) = 1.32$ if this separation corresponds to adjacent modes of even and odd ℓ . Both estimates are in poor agreement with our value of 1.08 for the stellar luminosity. However, in roAp stars the magnetic field of a few kG can change the pulsation frequency by 10–30 μHz , depending on latitudinal degree ℓ . The first demonstration that such large perturbations to the frequencies would occur was given by Cunha & Gough (2000), using a polytropic model. This was confirmed later, by Saio & Gautschi (2004), using a regular stellar model. Thus the resulting frequency separation can be quite different from those expected in a star without a magnetic field. Additional modelling is required for correct mode identification, but at present we rather favour adjacent modes. The results of our RV analysis presented here and by Ryabchikova et al. (2007b) will be used in pulsational modelling of 33 Lib in the same manner as was done for the roAp star HD 24712 (Saio et al. 2010). The fact that the frequency solution derived from our extensive 2009 spectroscopic data perfectly fits the UVES data obtained in 2004 allows us to use these more precise data for modelling. This work is in progress.

As in many other recent studies of RV variations in roAp stars, one can interpret the measurements of RV amplitude and phase in terms of outward propagation of pulsation waves in a chemically stratified stellar atmosphere. The phase behaviour derived from spectroscopic studies of roAp stars is usually interpreted as resulting from the presence of running or standing waves in the atmosphere. The pulsation properties of 33 Lib as well as 10 Aql are of considerable interest because these are the only roAp stars with clear signatures of a radial node in the upper atmosphere – the existence of pulsation zeros in the amplitude diagram accompanied by phase jumps in the phase diagram. A star’s pulsational behaviour on the phase-amplitude diagram may be interpreted as a superposition of standing and running pulsation waves mimicking an inwardly propagating wave, as discussed by Sousa & Cunha (2008a,b).

In the presence of a magnetic field, the surface boundary layer can be divided into two regions, one where the magnetic pressure is comparable to the gas pressure, so-called the coupling region, and one where the magnetic pressure is much larger than the gas pressure, which is the magnetically dominated region. The visual superposition of the line-of-sight projections of the acoustic and magnetic components, when integrated over the stellar region, may possibly result in the appearance of a ‘false node’ (Sousa & Cunha 2011). At the same time, the same behaviour of the phase and amplitude derived from lines that are sensitive to deeper regions of the atmosphere (say the base of the photosphere) may still reflect the presence of a real pulsation node (Sousa & Cunha 2011).

2D numerical simulations by Khomenko & Kochukhov (2009) presented the most complete theoretical picture to date of the propagation of magnetoacoustic waves in roAp stars. This non-linear magnetohydrodynamic study demonstrated the pseudo-node formation phenomenon for certain combinations of viewing geometries and pulsation periods, although the occurrence of this effect in the upper atmospheric layers was somewhat less common than in the analytical results by Sousa & Cunha. Among all the parameter combinations explored by Khomenko & Kochukhov (2009), the node in the upper atmosphere appears only for relatively short pulsation periods, not unlike those observed in 33 Lib, and highly inclined magnetic fields. The latter condition is compatible with the large horizontal to radial magnetic field component ratio inferred by Ryabchikova, Kochukhov & Bagnulo (2008) from spectrum synthesis modelling of Zeeman-resolved spectral lines.

At the same time, the study by Khomenko & Kochukhov (2009) emphasized the importance of realistic treatment of the thermodynamic structure of the stellar atmosphere. Any rapid temperature or density variation with height leaves an imprint on the depth dependence of the pulsational amplitude and phase. For example, the density inversion due to hydrogen ionization in the lower atmosphere of late-A stars results in a sharp enhancement of the temperature and density perturbations at $\log \tau_{5000} = 0$. Similarly, the pulsation signature of the temperature inversion due to high-lying rare-earth clouds (Shulyak et al. 2010) may contribute to the RV variability of the Nd and Pr lines observed in the spectrum of 33 Lib. The propagation of pulsation waves through the anomalous upper atmosphere could also be responsible for the appearance of harmonic oscillations, for which no credible theoretical explanation has been suggested so far.

A detailed study of chemical stratification and atmospheric structure of 33 Lib, coupled with numerical modelling of the magnetoacoustic wave propagation, is required for a secure interpretation of pulsation results and detailed 3D asteroseismology of this key roAp star.

ACKNOWLEDGMENTS

MS and TR acknowledge support by the Presidium RAS programme, by research grants from RFBI (08-02-00469, 09-02-00002) and by the Russian Federal Agency on Science and Innovation (no. 02.740.11.0247). MH and WWW acknowledge support by the Austrian Science Fonds (FWF P22691-N16). OK is a Royal Swedish Academy of Sciences Research Fellow supported by grants from the Knut and Alice Wallenberg Foundation and the Swedish Research Council. GW acknowledges support from the Natural Science and Engineering Research Council of Canada (NSERC) and the Department of National Defence (Canada) Academic Research Programme. DS acknowledges support from Deutsche Forschungsgemeinschaft (DFG) Research Grant RE1664/7-1.

REFERENCES

- Adelman S. J., Pyper D. M., Shore S. N., White R. E., Warren W. H., Jr, 1989, *A&AS*, 81, 221
- Balmforth N. J., Cunha M. S., Dolez N., Gough D. O., Vauclair S., 2001, *MNRAS*, 323, 362
- Bruntt H. et al., 2009, *MNRAS*, 396, 1189
- Cunha M., Gough D., 2000, *MNRAS*, 319, 1020
- Donati J.-F., Semel M., Carter B. D., Rees D. E., Cameron A. C., 1997, *MNRAS*, 291, 658
- Gruberbauer M., Saio H., Huber D., 2008, *A&A*, 480, 223
- Guenther D. B. et al., 2008, *ApJ*, 687, 1448
- Huber D. et al., 2008, *A&A*, 483, 239
- Jamar C., Macau-Hercot D., Monfils A., Thompson G. I., Houziaux L., Wilson R., 1976, *Ultraviolet Bright-star Spectrophotometric Catalogue. A Compilation of Absolute Spectrophotometric Data Obtained with the Sky Survey Telescope (S2/68) on the European Astronomical Satellite TD-1*. ESA, Noordwijk
- Khan S., Shulyak D., 2006, *A&A*, 448, 1153
- Khomenko E., Kochukhov O., 2009, *ApJ*, 704, 1218
- Kochukhov O., 2006, *A&A*, 446, 1051
- Kochukhov O., 2007, in Kudryavtsev D. O., Romanyuk I. I., Nizhnij Arkhyz, eds, *Physics of Magnetic Stars. Special Astrophysical Observatory, RAS*, p. 109
- Kochukhov O., Bagnulo S., 2006, *A&A*, 450, 663
- Kochukhov O., Ryabchikova T., 2001a, *A&A*, 374, 615
- Kochukhov O., Ryabchikova T., 2001b, *A&A*, 377, L22
- Kochukhov O., Tsymbal V., Ryabchikova T., Makaganyk V., Bagnulo S., 2006, *A&A*, 460, 831
- Kupka F., Piskunov N., Ryabchikova T. A., Stempels H. C., Weiss W. W., 1999, *A&AS*, 138, 119
- Kurtz D. W., 1982, *MNRAS*, 200, 807
- Kurtz D. W., 1983, *MNRAS*, 202, 1
- Kurtz D. W., 1991, *MNRAS*, 249, 468
- Kurtz D. W., Elkin V. G., Mathys G., 2005a, *MNRAS*, 358, L6
- Kurtz D. W., Handler G., Ngwato B., 2005b, *Inf. Bull. Var. Stars*, 5647, 1
- Kurtz D. W., Elkin V. G., Mathys G., 2006, *MNRAS*, 370, 1274
- Leblanc F., Monin D., Hui-Bon-Hoa A., Hauschildt P. H., 2009, *A&A*, 495, 937
- Lenz P., Breger M., 2005, *Commun. Asteroseismol.*, 146, 53
- Libbrecht K. G., 1988, *ApJ*, 330, L51
- Martinez P. et al., 1996, *MNRAS*, 282, 243
- Matthews J. M., Kurtz D. W., Martinez P., 1999, *ApJ*, 511, 422
- Michaud G., 1970, *ApJ*, 160, 641
- Mkrtrichian D. E., Hatzes A. P., Kanaan A., 2003, *MNRAS*, 345, 781
- Mkrtrichian D. E., Hatzes A. P., Saio H., Shobbrook R. R., 2008, *A&A*, 490, 110
- Panchuk V. E., Klochkova V. G., Yushkin M. V., Naidenov I. D., 2009, *J. Opt. Technol.*, 76, 87
- Piskunov N. E., Valenti J. A., 2002, *A&A*, 385, 1095
- Reegen P., 2007, *A&A*, 467, 1353
- Ryabchikova T., Piskunov N., Kochukhov O., Tsymbal V., Mittermayer P., Weiss W. W., 2002, *A&A*, 384, 545
- Ryabchikova T., Wade G. A., LeBlanc F., 2003, in Piskunov N., Weiss W. W., Gray D. F., eds, *Proc. IAU Symp. 210, Modelling of Stellar Atmospheres*. Astron. Soc. Pac., San Francisco, p. 301
- Ryabchikova T., Nesvacil N., Weiss W. W., Kochukhov O., Stütz C., 2004, *A&A*, 423, 705
- Ryabchikova T. et al., 2007a, *A&A*, 462, 1103
- Ryabchikova T., Sachkov M., Kochukhov O., Lyashko D., 2007b, *A&A*, 473, 907
- Ryabchikova T., Kochukhov O., Bagnulo S., 2008, *A&A*, 480, 811
- Sachkov M., Kochukhov O., Ryabchikova T., Huber D., Leone F., Bagnulo S., Weiss W. W., 2008a, *MNRAS*, 389, 903
- Sachkov M., Ryabchikova T., Gruberbauer M., Kochukhov O., 2008b, *Commun. Asteroseismol.*, 157, 363
- Saio H., Gautschi A., 2004, *MNRAS*, 350, 485
- Saio H., Ryabchikova T., Sachkov M., 2010, *MNRAS*, 403, 1729
- Savanov I. S., Kochukhov O. P., Tsymbal V. V., 2001, *Astrophys.*, 44, 206
- Shulyak D., Tsymbal V., Ryabchikova T., Stütz C., Weiss W. W., 2004, *A&A*, 428, 993
- Shulyak D., Ryabchikova T., Kildiyarova R., Kochukhov O., 2010, *A&A*, 520, A88
- Sousa S. G., Cunha M. S., 2008a, *MNRAS*, 386, 351
- Sousa J., Cunha M. S., 2008b, *Contri. Astron. Obser. Skalnaté Pleso*, 38, 453
- Sousa S. G., Cunha M. S., 2011, *MNRAS*, 414, 2576
- Tassoul M., 1980, *ApJS*, 43, 469
- van Leeuwen F., 2007, *A&A*, 474, 653
- Wade G. A., Ryabchikova T. A., Bagnulo S., Piskunov N., 2001, in Mathys G., Solanki S. K., Wickramasinghe D. T., eds, *ASP Conf. Ser. Vol. 248, Magnetic Fields Across the Herzprung-Russell Diagram*. Astron. Soc. Pac., San Francisco, p. 341
- Walker G. et al., *PASP*, 115, 1023

This paper has been typeset from a $\text{\TeX}/\text{\LaTeX}$ file prepared by the author.